Silicon-Based Integrated Optical Pressure Sensor Using Intermodal Interference between TM-like and TE-like Modes

Yuki Shirai[a], Takeshi Goto[a], Masashi Ohkawa*[b], Seishi Sekine[b], and Takashi Sato[b]

[a]Niigata University, Graduate School of Science and Technology
8050 Ikarashi 2-no-cho, Niigata 950-2181, Japan
[b]Niigata University, Faculty of Engineering
8050 Ikarashi 2-no-cho, Niigata 950-2181, Japan

ABSTRACT

A silicon-based integrated optical pressure sensor using an intermodal interference between the fundamental TM-like and TE-like modes is described. The sensor consists of a micromachined rectangular diaphragm and a straight polystyrene optical waveguide passing across the diaphragm. The use of the intermodal interference has the potential advantage of shortening the sensor length since it needs neither a Y-branch nor a 3-dB coupler. In the presence of the pressure difference on the diaphragm, the phase difference is yielded between the two guided modes by an anisotropic index change induced by the elasto-optic effect. The phase difference is finally transformed into a change in light intensity by an analyzing polarizer. We fabricated a sensor with a 1.2 mm×10 mm×20 μm diaphragm over which the waveguides were formed at 50 μm intervals. In the experiment, a linearly-polarized He-Ne laser beam at 633 nm was coupled to the two guided modes at equal intensity. The output intensity through a polarizer was sinusoidally changed at a period of 64 kPa, corresponding to a phase sensitivity of 98 mrad/kPa, for the waveguide nearest to the diaphragm edge. The measurement was carried out for other waveguide positions. The largest sensitivity was obtained for the waveguide nearest to the diaphragm edge as theoretically expected.

Keywords: integrated optics, intermodal interference, pressure sensor, silicon, diaphragm

1. INTRODUCTION

Since an integrated optical temperature sensor was first reported in 1981[1], many integrated optical sensors have been proposed and demonstrated[2-5]. The integrated optical sensors have several advantages such as compactness, lightness and alignment-free configuration and potentially efficient interaction between the lightwave and a measurand. For the integrated optical sensor, lithium niobate, silicon, glass and so on were used as substrates. Silicon is an attractive substrate not only because of its well-established electronic properties but also because of its excellent mechanical properties. Micromaching technology in silicon opened the way for micro-opto-mechanical devices. In the last decade, integrated optical sensors incorporated with micromechanical structures have attracted much attention due to the development of micromachining technologies.[6, 7] Several groups have demonstrated the integrated-optic interferometric pressure sensors employing micromachined diaphragms.[8-10] These sensors utilized phase-sensitive optical circuits, e.g. the Mach-Zehnder interferometer[8,9] and the ring resonator[10]. Our group has been developing glass-based and silicon-based integrated optical pressure sensors using the intermodal interference between the TM-like and TE-like modes.[11, 12] The use of the intermodal interference offers a potential advantage of a shortened sensor length since any waveguide branches or 3-dB directional couplers, which require a longer sensor length, are unnecessary. As an application of the silicon-based pressure sensor, we are particularly interested in blood pressure measurement, because the sensor has the following excellent features: immunity to electromagnetic interference, impossibility of electrical leak and minituarization feasibility. Incidentally, the sensitivity of the integrated optical pressure sensor with the diaphragm is theoretically known to have a strong dependence on the position of the sensing waveguide of the phase-sensitive optical circuit.[8, 11-13] Their relationship has not, however, been experimentally investigated. According to the theoretical prediction for the sensor based on the elasto-optic effect, the sensing waveguide should be placed along the longer side of the rectangular diaphragm to maximize the sensitivity. For design of the sensor, it is worthwhile to study how the sensitivity is dependent on the position of the waveguide across the diaphragm. We have experimentally examined the phase sensitivity of a silicon-based integrated optical pressure sensor using the intermodal interference. In this paper, the configuration of the pressure sensor, a principle of sensor operation, the

Integrated Optics Devices V, Giancarlo C. Righini, Seppo Honkanen, Editors,
Proceedings of SPIE Vol. 4277 (2001) © 2001 SPIE · 0277-786X/01/$15.00

theoretical result of the phase sensitivity versus the waveguide position, and the sensitivities of the fabricated sensor for several waveguide positions are described.

2. PRINCIPLE OF OPERATION

Fig.1 shows the integrated optical pressure sensor using the intermodal interference between the TM-like and TE-like modes. The sensor has a rectangular diaphragm as a pressure-sensitive mechanical structure and a straight optical waveguide across the diaphragm. The waveguide guides the lowest-order TM-like and TE-like modes. The diaphragm is distorted when a pressure difference is applied to the diaphragm. The distortion causes strain, which produces a change in the refractive index of the diaphragm by the elasto-optic effect. The index change yields phase retardation in the lightwave, which propagates in the waveguide on the diaphragm. When the phase retardation is dependent on the guided modes, the phase difference between the two modes is also a function of the applied pressure. To detect the phase difference, the sensor is placed in a pair of crossed polarizers as shown in Fig.2. The input polarizer is oriented at 45° with respect to the polarization of each guided mode. The light beam through the input polarizer is coupled to the TM-like and TE-like modes at equal intensities. At the end of the waveguide, the lightwave has linear, elliptic or circular polarization, corresponding to the induced phase difference between the two guided modes. The crossed output polarizer converts the polarization-modulated light into intensity-modulated light. The intensity of the beam passing through the output polarizer sinusoidally changes with the applied pressure. Therefore, the pressure applied to the diaphragm can be determined from the output intensity of the sensor system with the polarizers.

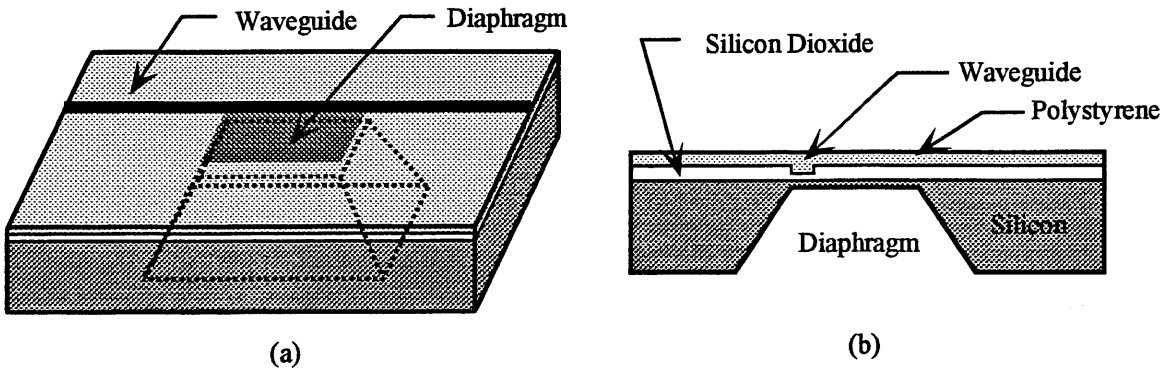

Fig.1 (a) Schematic drawing of the integrated optical pressure sensor using intermodal interference, and (b) a cross-sectional view.

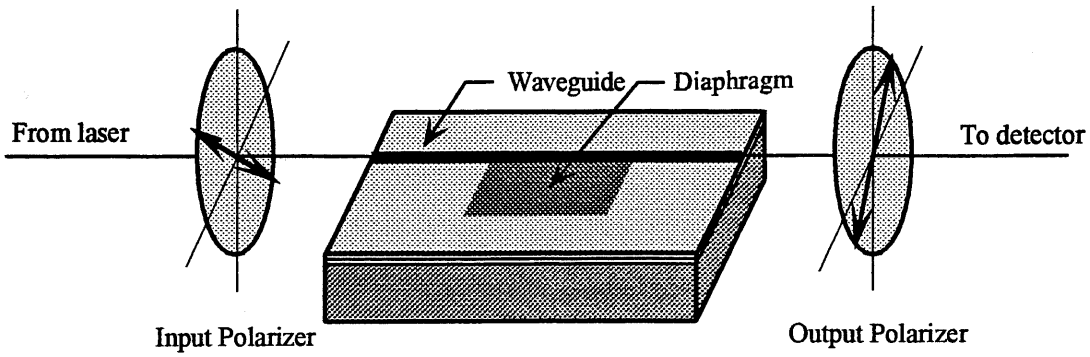

Fig.2 A sensor system using a pair of crossed polarizers to detect the induced phase difference between the two orthogonal guided modes.

3. THEORETICAL ANALYSIS

3.1. Mathematical Description

Fig 3 shows a rectangular diaphragm with an area of $a \times b$ and a thickness of t, as assumed in this section. The y-z plane lies in the middle plane between the two surfaces of the diaphragm and the z-axis is parallel to the waveguide. The x-axis is perpendicular to the plate surface. Deflection w of the diaphragm, or displacement from the equilibrium position, due to the uniformly applied pressure q, is obtained from the differential equation:

$$\frac{\partial^4 w}{\partial y^4} + 2\frac{\partial^4 w}{\partial y^2 \partial z^2} + \frac{\partial^4 w}{\partial z^4} = \frac{q}{D}, \tag{1}$$

where D is flexural rigidity, defined as $D = Yt^3/12(1-\rho^2)$. Y and ρ are the modulus of elasticity and the Poisson's ratio, respectively. From the obtained deflection, the distribution of stress T in the diaphragm is derived.[13] Next, the strain distribution S is calculated assuming that Hooke's law applies.[13] The change of dielectric constant $\Delta\varepsilon$ induced by the strain is given by

$$\Delta\varepsilon_i = -\varepsilon^2 p_{ij} S_j, \ (i, j = 1\text{-}6), \tag{2}$$

where p_{ij} denotes each component of the elasto-optic tensor. The strain has six components which are divided into two kinds of strain: the normal strains in the x, y and z directions with subscripts 1, 2 and 3 respectively, and the shearing strains with subscripts 4, 5, and 6. The changes $\Delta\varepsilon_1$ and $\Delta\varepsilon_2$ give the different phase retardations to the two guided waves traveling on the diaphragm. The amount of phase difference $\Delta\phi$ between them is expressed as

$$\Delta\phi = \Delta\phi_{TM} - \Delta\phi_{TE}, \tag{3}$$

where

$$\Delta\phi_{TM} \approx \int_{-b/2}^{b/2} \left(\frac{\omega\varepsilon_0}{4} \int_{-a/2}^{a/2} \int_{-t/2}^{t/2} E_x(x,y) \Delta\varepsilon_1(x,y,z) E_x^*(x,y) dx dy \right) dz \tag{4}$$

and

$$\Delta\phi_{TE} = \int_{-b/2}^{b/2} \left(\frac{\omega\varepsilon_0}{4} \int_{-a/2}^{a/2} \int_{-t/2}^{t/2} E_y(x,y) \Delta\varepsilon_2(x,y,z) E_y^*(x,y) dx dy \right) dz. \tag{5}$$

In these equations, ω is the angular frequency of the light, ε_0 is the permittivity of vacuum, and $*$ indicates complex conjugate. Also, E_x and E_y are the power-normalized x-directed electric field component of the TM-like mode and the y-directed electric field component of the TE-like mode, respectively. The intensity after the output polarizer is derived from the phase difference calculated in Eq. (3). The phase sensitivity, defined as the resultant phase difference per unit pressure, is used as an important measure to evaluate the sensor performance. The halfwave pressure, which yields the phase difference of π rad, is also used for the evaluation in this study.

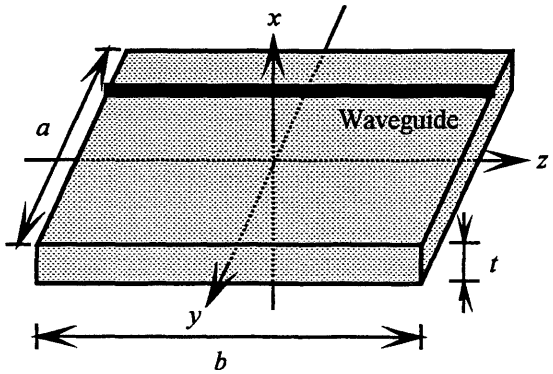

Fig.3 Illustration of the rectangular diaphragm assumed in the calculations.

The theoretical calculation described above should be carried out using the mechanical and optical parameters of the materials which comprise the sensor. We have yet to get those of polystyrene, which is the material for the guided layer of the fabricated sensor described below. So, in the calculation, the parameters of fused silica were used instead of those of polystyrene. The numerical result obtained by using the parameters of fused silica would quantitatively hold true for the sensor using a polystyrene waveguide.

3.2. Theoretical Result of Sensitivity versus Waveguide Position

The induced index change is not uniformly distributed inside the diaphragm, so that the induced phase difference is dependent on the position of the waveguide passing across the diaphragm. The phase sensitivities, that is, the phase differences per unit pressure, were calculated as a function of the waveguide position. In the calculation, the pressure was assumed to be uniformly applied over the diaphragm with all the edges clamped. Also, the wavelength of the guided light was 633 nm. Fig.4 shows a calculated result in which the ratio of the length and width of the diaphragm is taken as a parameter. The phase sensitivities are normalized to be at unity at $y = \pm a/2$ for each aspect ratio. The phase sensitivities have a maximum value when the waveguide is located along the side of the diaphragm, that is, at $y = \pm a/2$. In other words, the side of the diaphragm is the best waveguide position to maximize the sensitivity of the sensor.

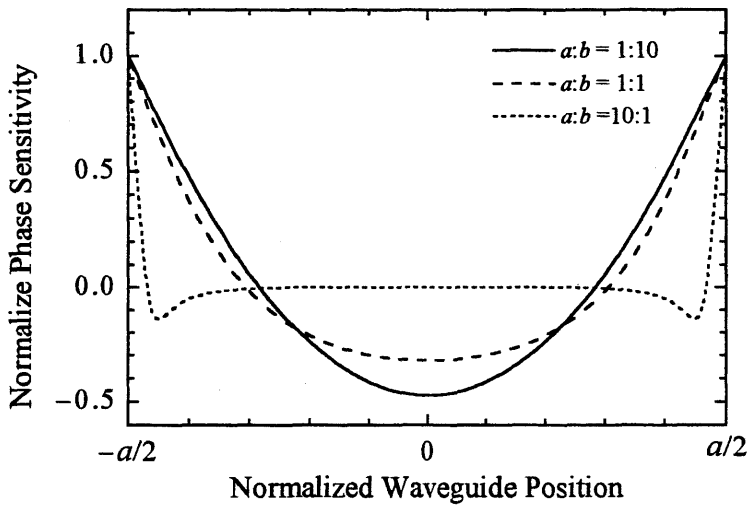

Fig.4 The relations between the normalized phase sensitivity and the waveguide position in the y-direction. The waveguide positions of $\pm a/2$ represent the waveguide along the side of the diaphragm, whereas a position of 0 corresponds to the center of the diaphragm.

4. EXPERIMENT

4.1. Fabrication

Fig.5 shows a schematic diagram of the fabricated sensor and a cross-section of the ridge-type waveguide. The waveguide was designed to become single-mode using the effective index method. The sensor had 25 waveguides spaced at 50 μm to determine how phase sensitivity is related to waveguide position. In the fabrication, a silicon dioxide layer was first formed on both sides of the substrate by thermal oxidation. The SiO_2 layer of the bottom surface was selectively removed by an etchant of buffered HF acid using a patterned photoresist as an etching mask. Then, the exposed silicon was anisotropically etched by KOH to produce the diaphragm. The area of the diaphragm was 1.2mm × 10 mm and its thickness was 20 μm. After the diaphragm fabrication, the silicon dioxide was removed from the substrate and was regrown 1 μm, sufficient to make the radiation loss of the TM-like and TE-like modes into the substrate negligible. Then, shallow grooves of about 10 μm wide and 0.1 μm deep were formed on the silicon dioxide layer parallel to the diaphragm side using buffered HF acid. The polystyrene layer was spin-coated, and its thickness at the grooves was 1.1 μm.

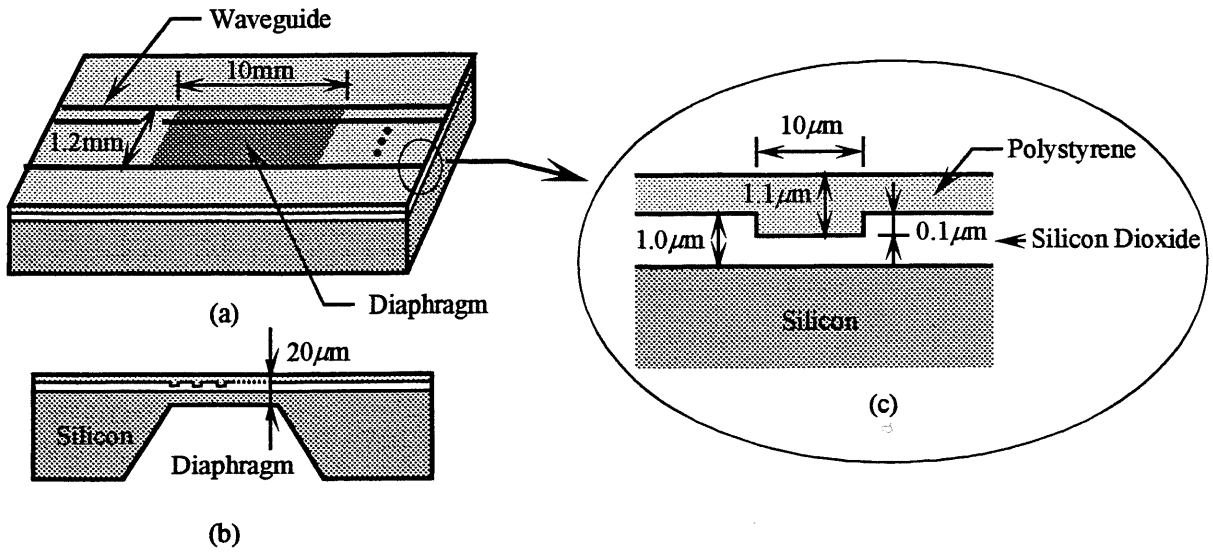

Fig.5 (a) Schematic drawing of the fabricated sensor, (b) its cross-sectional view, and (c) the cross-section of the ridge-type waveguide. The width of the polystyrene channel waveguides was 10 μm, and the dimensions of the diaphragm are 1.2 mm× 10 mm×20 μm.

4.2. Measurement of Phase Sensitivity

Fig.6 illustrates the experimental setup to measure output intensity versus applied pressure. The sensor was tested using a linearly-polarized He-Ne laser at 633 nm. The polarization of the laser beam was set at 45° to the sensor surface, so that the input polarizer shown in Fig.2 was not necessary in this experiment. The sensor was connected to a 100 ml syringe by a silicone tube in order to apply pressure to the diaphragm. Pulling and pushing the plunger of the syringe caused a pressure difference, ranging from –50 kPa to 40 kPa, on the diaphragm. The positive value represents a pressure in the etched hole

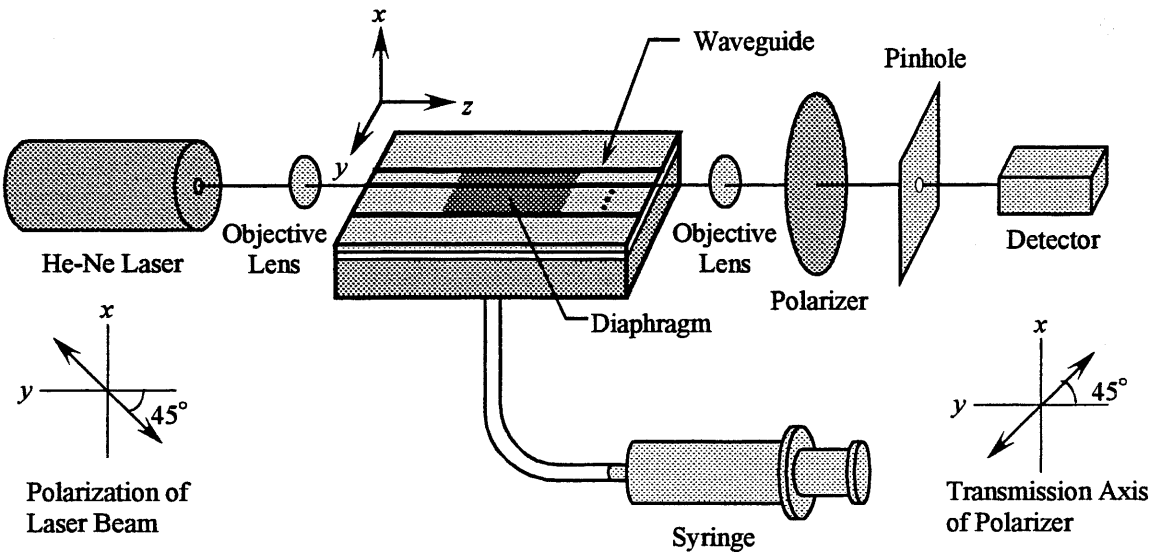

Fig.6 The arrangement of the sensor system.

being higher than that in the atmosphere. Fig.7(a) shows the experimental result for the waveguide nearest to the diaphragm edge. Also, Fig.7(b) and (c) indicate the results for the waveguides located apart from the waveguide of Fig.7(a) by 0.2 mm and 0.55 mm inside the diaphragm, respectively. The waveguide of Fig.7(c) was placed near the center of the diaphragm since the width of the diaphragm was 1.2 mm. The solid line in each figure indicates a computer projection of the experimental data. A half period of the output intensity is called the halfwave pressure, and determines the dynamic range

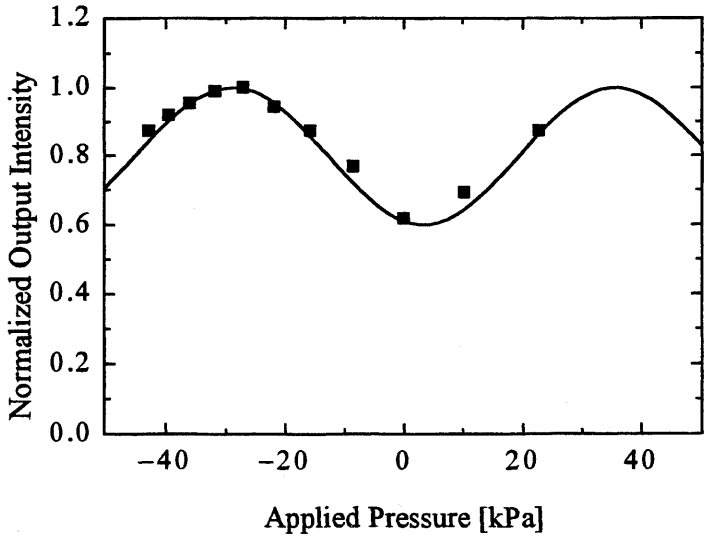

Fig.7(a) The experimental result and the best fit sinusoidal curve for the waveguide nearest to the diaphragm edge. The phase sensitivity was 98 mrad/kPa, corresponding to a halfwave pressure of 32 kPa.

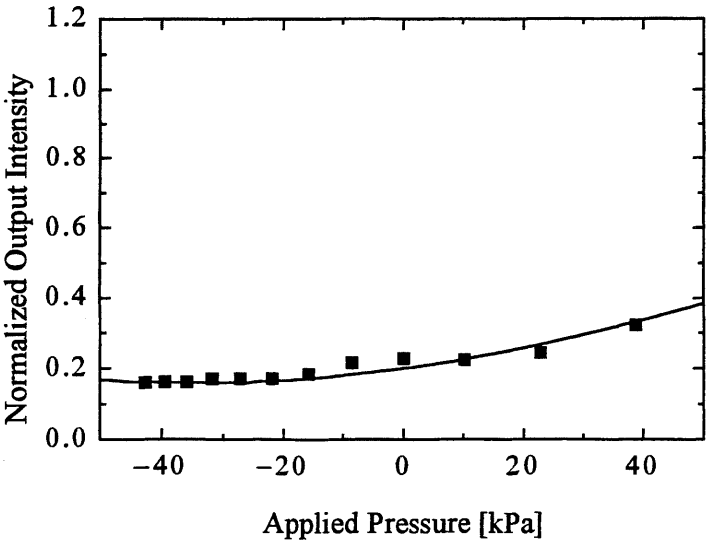

Fig.7(b) The experimental result for the waveguide apart from the waveguide of Fig.7(a) by 0.2 mm inside the diaphragm. The phase sensitivity was 13 mrad/kPa, corresponding to a halfwave pressure of 240 kPa.

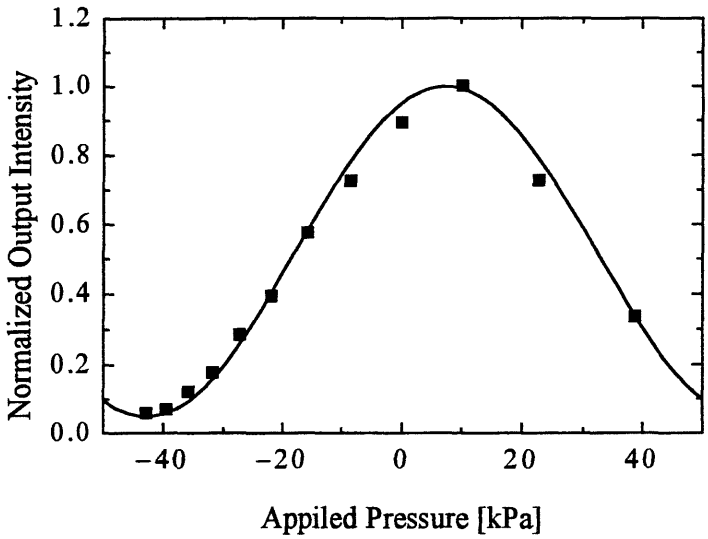

Fig.7(c) The experimental result for the waveguide apart from the waveguide of Fig.7(a) by 0.55 mm inside the diaphragm. The waveguide position was almost center since the diaphragm width was 1.2 mm. The phase sensitivity was 63 mrad/kPa, corresponding to a halfwave pressure of 50 kPa

in which the output intensity and the applied pressure show a one-to-one correspondence. From the Fig.7(a), the halfwave pressure is evaluated to be 32kPa, corresponding to a phase sensitivity of 98 mrad/kPa. The phase sensitivities are 13 mrad/kPa and 63 mrad/kPa for Fig.7(b) and (c), respectively. Moreover, it is found from Fig.7(a)-(c) that the extinction ratios are less than 10dB except in Fig.7(c), and the initial phase differences exist between the two guided modes. The low extinction ratios were attributed to the stray light through the pinhole. The non-zero initial phase differences arose from the difference between the effective indices of the guided modes. If the effective index difference is relatively large, the initial phase difference can be adjusted by changing the waveguide length.
If blood pressure measurement is considered as an application of this sensor, the halfwave pressure of 32 kPa for the waveguide nearest to the diaphragm edge would be sufficient. The sensor must, however, be further miniaturized while maintaining the sensitivity in order to be incorporated into a catheter.

5. CONCLUSIONS

The phase sensitivity of a silicon-based optical pressure sensor using the intermodal interference was experimentally examined. The sensitivity of the sensor was found to be dependent on the position of the waveguide on the diaphragm. The largest sensitivity of 98 mrad/kPa was obtained for the waveguide located nearest to the diaphragm edge. The sensitivity is sufficient for blood pressure measurement although the sensor must be further miniaturized. In addition, to miniaturize the entire sensor system, the objective and the polarizer in the experimental setup must be replaced with polarization-maintaining fibers attached to the two endfaces of the sensor. If a mirror film is put onto an endface instead of the fiber, the other endface can used as the input and output port, thus making it possible to realize a compact sensor with one pigtail polarization-maintaining fiber.

ACKNOWLEDGMENTS

This work is supported by a Grant-in-Aid for Scientific Research (No.12650339) from the Japan Society for the Promotion of Science.

REFERENCES

1. L. M. Johnson, G. W. Pratt, and F. J. Leonberger, "Integrated-optical temperature sensor," *in Technical Digest, Third International Conference on Integrated Optics and Optical Fiber Communication*, pp.130-131, 1981.
2. M. Izutsu, A. Enokihara, and T. Sueta, "Optical-waveguide microdisplacement sensor," Electron. Lett., **18**, pp.867-868, 1982.
3. A. Enokihara, M. Izutsu, and T. Sueta, "Integrated-optic fluid sensor using heat transfer," Appl. Opt., **27**, pp.109-113, 1988.
4. H. Toda, K. Kasazumi, M. Haruna, and T. Nishihara, "An optical integrated circuit for time-division 2-D velocity measurement," J. Lightwave Technol., **7**, pp.364-367, 1989.
5. D. Jestel, A. Baus, and E. Voges, "Integrated-optic interferometric microdisplacement sensor in glass with thermooptic phase modulator," Electron. Lett., **26**, pp.1144-1145, 1990.
6. M. Tabib-Azar, and G. Beheim,"Modern trends in microstructures and integrated optics for communication, sensing, and actuation," Opt. Eng., **36**, pp.1307-1318, 1997.
7. E. Ollier, P. Philippe, C. Chabrol, and P. Mottier, "Micro-opto-mechanical vibration sensor integrated on silicon," J. Lightwave Technol., **17**, pp.26-29, 1999.
8. M. Ohkawa, M. Izutsu, and T. Sueta, "Integrated optic pressure sensor on silicon substrate," Appl. Opt., **28**, pp.5153-5157, 1989.
9. H. Porte, V. Gorel, S. Kiryenko, J. Goedgebuer, W. Daniau, and P. Blind, "Imbalanced Mach-Zehnder interferometer integrated in micromachined silicon substrate for pressure sensor," J. Lightwave Technol., **17**, pp.229-233, 1999.
10. G. N. De Brabander, J. T. Boyd, and G. Beheim, "Integrated optical ring resonator with micromechanocal diaphragm for pressure sensing," IEEE Photon. Technol. Lett., **6**, pp.671-673, 1994.
11. M. Ohkawa, K. Hasebe, C. Nishiwaki, S. Sekine, and T. Sato, "Integrated optical pressure sensor using intermodal interference between two mutual orthogonal guided-modes," Optical Review, **7**, pp.144-148, 2000.
12. M. Ohkawa, C. Nishiwaki, K. Hasebe, S. Sekine, and T. Sato, "Glass-based integrated optic pressure sensors with a Mach-Zehnder interferometer and with an intermodal interferometer," Proc. of SPIE, **3936**, pp.309-318, 2000.
13. M. Ohkawa, T. Abe, S. Sekine, and T. Sato, "Integrated optic micropressure sensor using ring resonator," Electronics and Communications in Japan, **79**, pp.1-10, 1996.

* Correspondence: E-mail: ohkawa@eng.niigata-u.ac.jp; Telephone & Fax: +81-25-262-6734